WILEY-VCH

ADVANCED MATERIALS

Supporting Information

Programmable dual regime spray for large-scale and custom-designed electronic textiles

Taehoo Chang, Semih Akin, Min Ku Kim, Laura Murray, Bongjoong Kim, Seungse Cho, Sena Hur, Sengul Teke, Laurent Couetil, Martin Byung-Guk Jun*, Chi Hwan Lee**

This PDF file includes:

Experimental Section

Figure S1 to S22

Other Supplementary Materials for this manuscript include the following:

Movies S1 to S3

Experimental Section

Overcoating process. The as-sprayed fabrics were immersed in an electroless Cu plating bath at room temperature for 6 hours. The plating bath was composed of 18 g L^{-1} of copper (II) sulfate pentahydrate ($CuSO_4 \cdot 5H_2O$; ≥ 98%; Sigma-Aldrich), 48 g L^{-1} of ethylenediaminetetraacetic acid (EDTA; ≥ 98%; Sigma-Aldrich), 45 g L^{-1} sodium hydroxide (NaOH; ≥ 97%; Fisher Chemical), 18 ml L^{-1} of hydrochloric acid (HCl; 1 N; Fisher Chemical), 200 mg L^{-1} of potassium hexacyanoferrate (II) trihydrate ($K_4Fe(CN)_6 \cdot 3H_2O$; ≥ 99.9%; Sigma-Aldrich), and 20 ml L^{-1} of formaldehyde (HCHO; 37% aqueous solution; Fisher Chemical). The fabrics were rinsed with deionized water and dried at room temperature. The Cu-plated conducting lines in the fabrics were covered with an Ecoflex overcoat (Ecoflex™ 00-30; Smooth-On) using a three-axis CNC router in a pre-programmed manner. The Ecoflex overcoat was cured at room temperature. The areas of recording electrodes were then coated with Au in a brush-type electroplating solution (24 K brush gold gel solution, Gold Plating Services). The resulting fabrics were rinsed in water for 20 minutes and dried in air. Lastly, standard snap button ends glued using a waterproof textile adhesive (Liquid Stitch) at the end of interconnection lines.

Computational fluid dynamics (CFD) modeling. The flow domain was discretized (meshed) using hexahedral elements with a cell number of 4,138,825. The boundary conditions for mass flow rate were applied to both atomized droplet air flow (i.e., 6.5×10^{-5} kg sec^{-1}) and central air flow (i.e., 2.2×10^{-5} kg sec^{-1}). An adiabatic wall with a no-slip boundary condition was used at the whole side surface of the dual regime spray system. At the nozzle exit, the pressure outlet boundary condition was used and set to atmospheric pressure (i.e., 1 bar). Standard k-ε turbulence model was used to model the cyclone effects in the mixing chamber. The turbulent intensity and viscosity ratio were set as 5% and 10%, respectively. The flow domain was solved in steady-state conditions. The

governing equations presented below for a steady compressible flow were solved using the Ansys-Fluent Version 19.1 software.

Continuity equation:

$$\boldsymbol{\nabla}.(\boldsymbol{\rho}\vec{\boldsymbol{u}}) = \mathbf{0} \quad (1)$$

Momentum equation:

$$\boldsymbol{\nabla}.(\boldsymbol{\rho}\vec{\boldsymbol{u}}\vec{\boldsymbol{u}}) = -\boldsymbol{\nabla p} + \boldsymbol{\nabla}.(\boldsymbol{\mu}\boldsymbol{\nabla}\vec{\boldsymbol{u}}) \quad (2)$$

Turbulent kinetic energy (TKE) equation:

$$\frac{\partial(\rho k u_i)}{\partial x_i} = \frac{\partial}{\partial x_j}\left[\frac{\mu_t}{\sigma_k}\frac{\partial k}{\partial x_j}\right] + 2\mu_t E_{ij}E_{ij} - \rho\varepsilon \quad (3)$$

Rate of dissipation equation:

$$\frac{\partial(\rho\varepsilon v_i)}{\partial x_i} = \frac{\partial}{\partial x_j}\left[\frac{\mu_t}{\sigma_\varepsilon}\frac{\partial \varepsilon}{\partial x_j}\right] + 2C_{1\varepsilon}\frac{\varepsilon}{k}\mu S_{ij}S_{ij} - C_{2\varepsilon}\rho\frac{\varepsilon^2}{k} \quad (4)$$

$$\mu_t = \rho C_\mu \frac{k^2}{\varepsilon} \quad (5)$$

where μ and ρ are the viscosity (Pa s) and density (kg m^{-3}) of air, $\boldsymbol{\mu}$ (m sec^{-1}) is the velocity, g is the gravitational constant, S_{ij} is the fluid strain rate sensor, and the turbulence model constants are $C_{\varepsilon 1} = 1.44$, $C_{\varepsilon 2} = 1.92$, $C_\mu = 0.09$, $\sigma_k = 1.0$, and $\sigma_\varepsilon = 1.3$, respectively. The contours of the air velocity inside and outside of the nozzle with and without the central air flow were obtained from numerical simulations. The results obtained from the CFD modeling were used to better focus the spray flow at a focal plane.

Finite element modelling (FEM) analysis. Three-dimensional FEM was performed using the Abaqus standard package to understand the underlying mechanics of a Lycra fabric under uniaxial tension. In this simulation, the Lycra fabric was modeled by 8-node three-dimensional solid elements (C3D8R) with the experimentally measured mechanical modulus (E = 2.3 kPa). The boundary conditions of displacement were applied to produce uniaxial loads for the strains of 25% and 50%.

Air flow recording. A horse was tethered in a temperature-controlled stock at 20 ºC. A pneumotachometer (#4 Fleisch, EMKA Technologies) was inserted in a facemask placed on the muzzle of the horse and coupled to a differential pressure transducer (DP-/45-14, Validyne Engineering) by two identical Teflon catheters to record airflow. The output signals from the pressure transducers were recorded simultaneously by the Pulmonary Mechanics Analyzer (XA version, Buxco Electronics, Sharon, CT).

Post-data processing. The recorded ECG and EMG data were digitally filtered at the time of recording using a data acquisition software (BioCaptureTM; GLNeuroTech Inc). A MATLAB code was used for post-data processing. The spectrograms were generated using a spectrogram function within the MATLAB library with a window of 500 while the number of overlapped samples was set at 63.

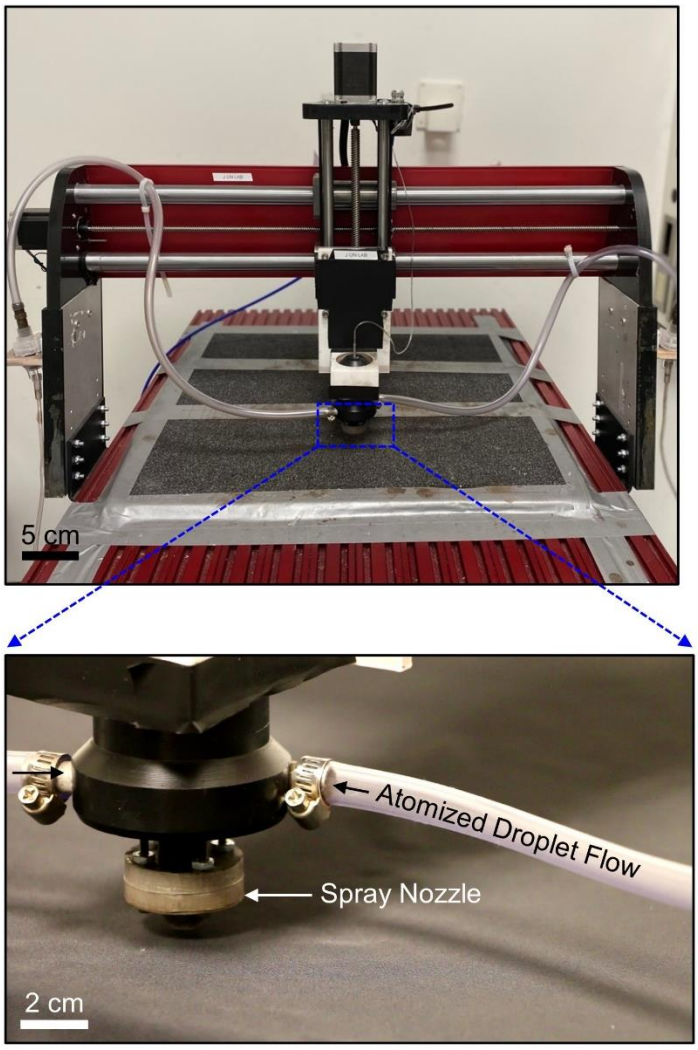

Figure S1. Representative photographs of the entire setting of the dual regime spray process.

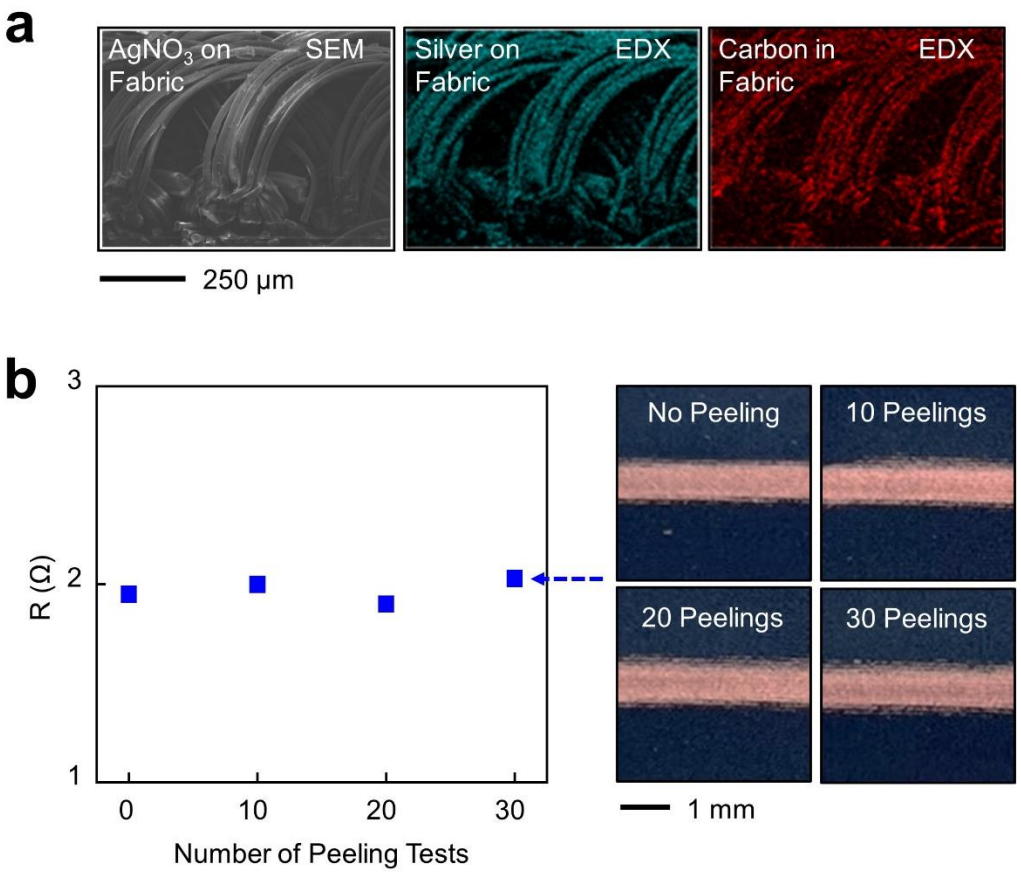

Figure S2. (a) Cross-sectional SEM and EDX images of the as-sprayed $AgNO_3$ nanoparticles on a Lycra fabric. (b) Resistance of the Cu overcoat following multiple peeling tests of the as-sprayed $AgNO_3$ nanoparticles using a Scotch tape (3M Inc).

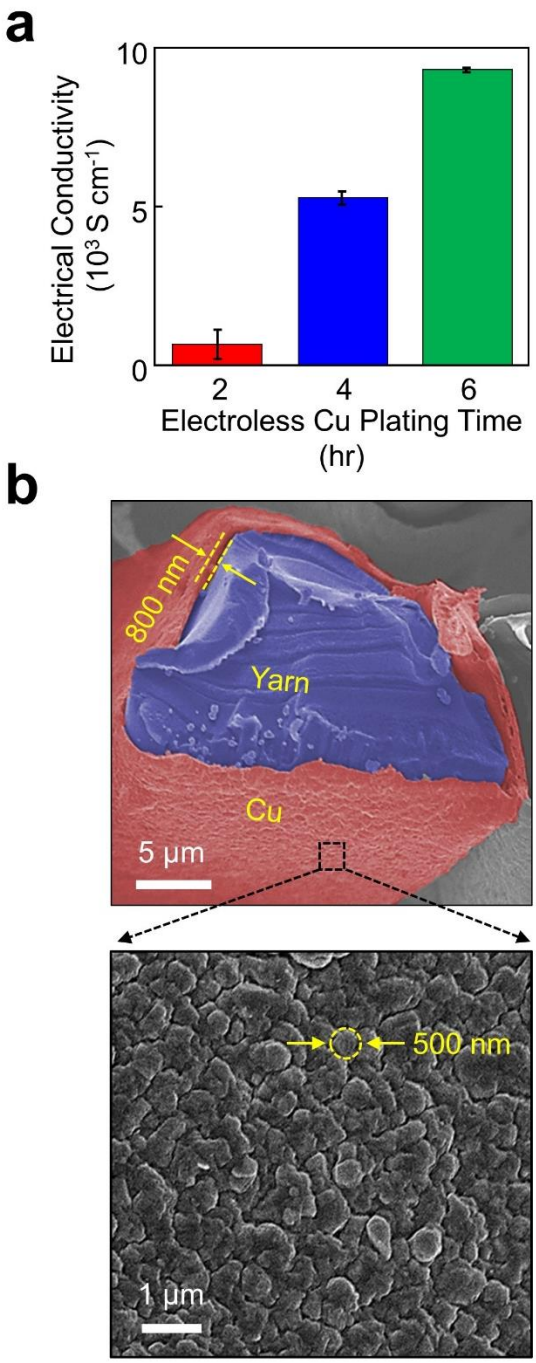

Figure S3. (a) Electrical conductivity of the Cu overcoat in a Lycra fabric as a function of electroless Cu plating time. (b) SEM images of the Cu overcoat in a Lycra fabric.

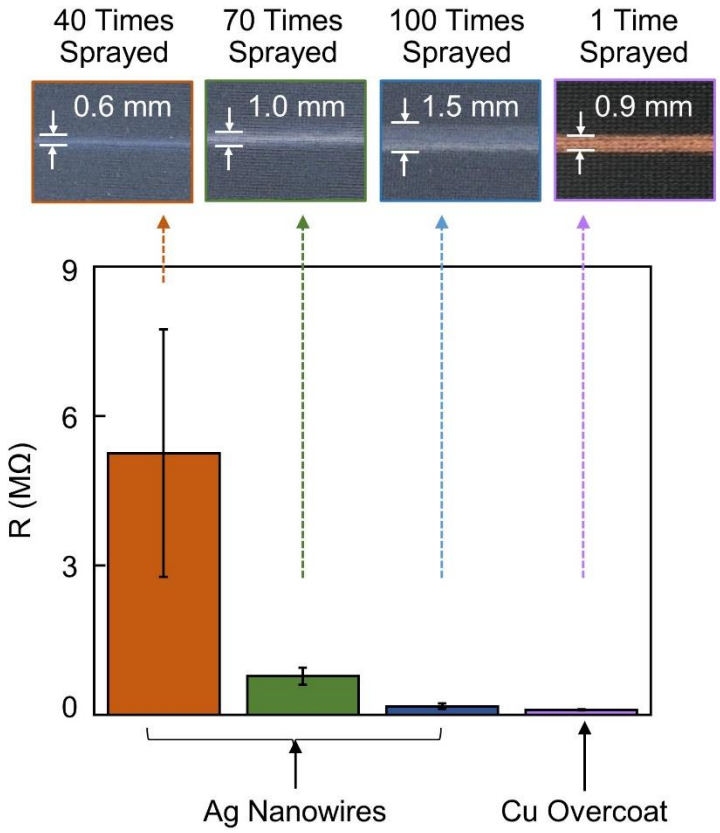

Figure S4. Resistance of the multiple times sprayed Ag nanowires into a Lycra fabric as compared to the one-time sprayed $AgNO_3$ nanoparticles with a Cu overcoat. The inset images indicate the spray resolution (i.e., line width) of each group.

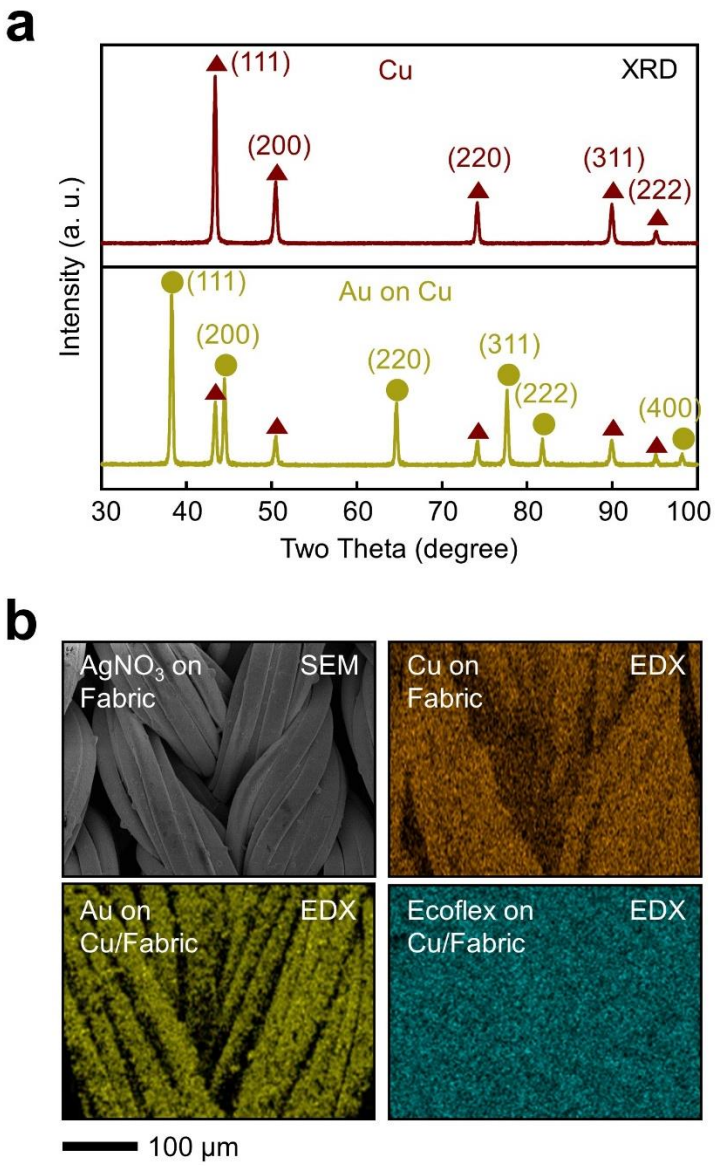

Figure S5. (a) XRD spectra of the Cu and Au overcoats in a Lycra fabric. (b) EDX-SEM mapping analysis of the sprayed $AgNO_3$ nanoparticles (left top panel), Cu overcoat (right top panel), Au overcoat (left bottom panel), and Ecoflex overcoat (right bottom panel) in a Lycra fabric.

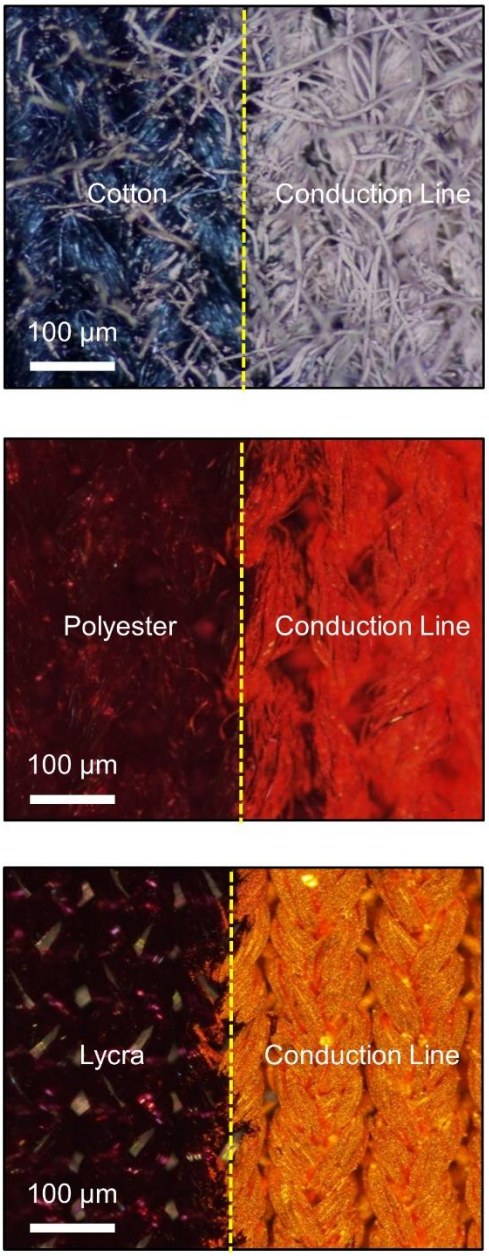

Figure S6. Microscope images of a sprayed conduction line in a cotton, polyester, and Lycra fabric from the top.

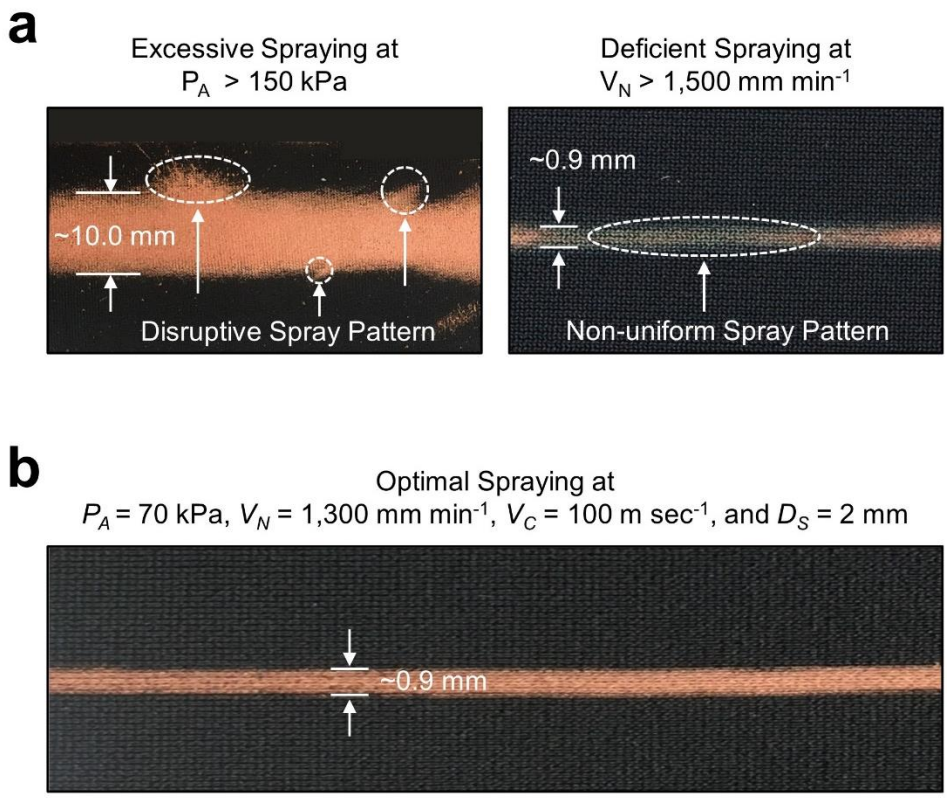

Figure S7. (a) Photographs of the excessively (left panel) and deficiently (right panel) sprayed conducting lines. (b) Photograph of the optimally sprayed conducting line.

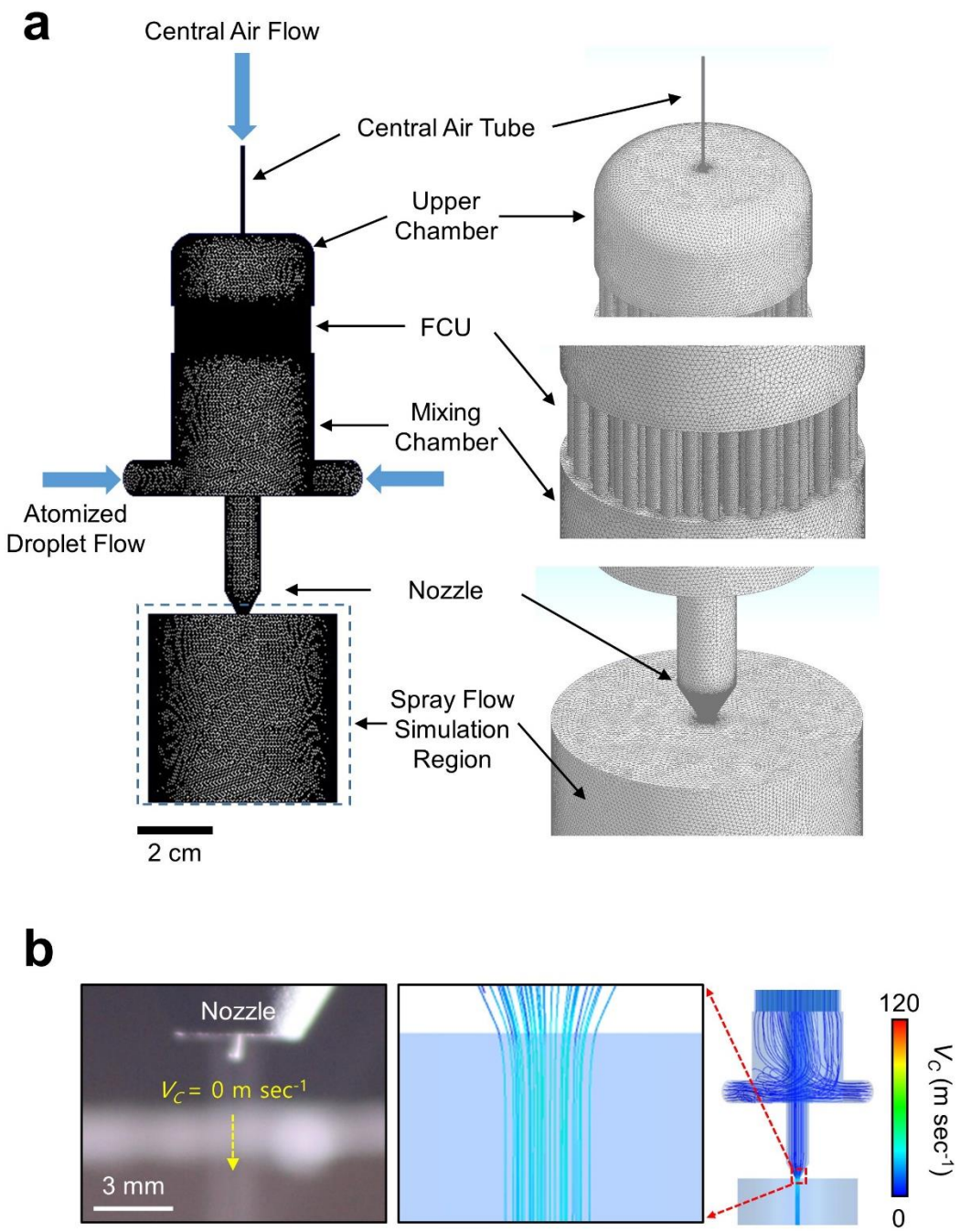

Figure S8. (a) Computational domain and local grid of the CFD modeling. (b) Representative experimental and CFD results of the spray flow when V_c = 0 m sec^{-1}.

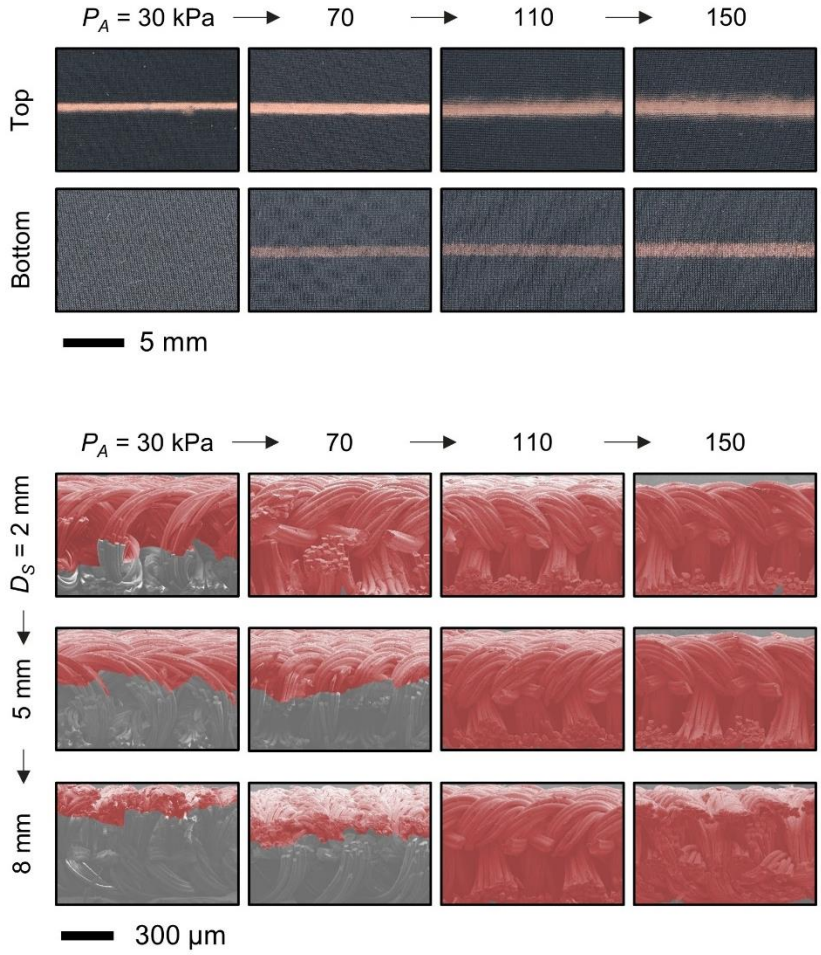

Figure S9. Representative microscope (top panel) and colored SEM images (bottom panel) of a test unit.

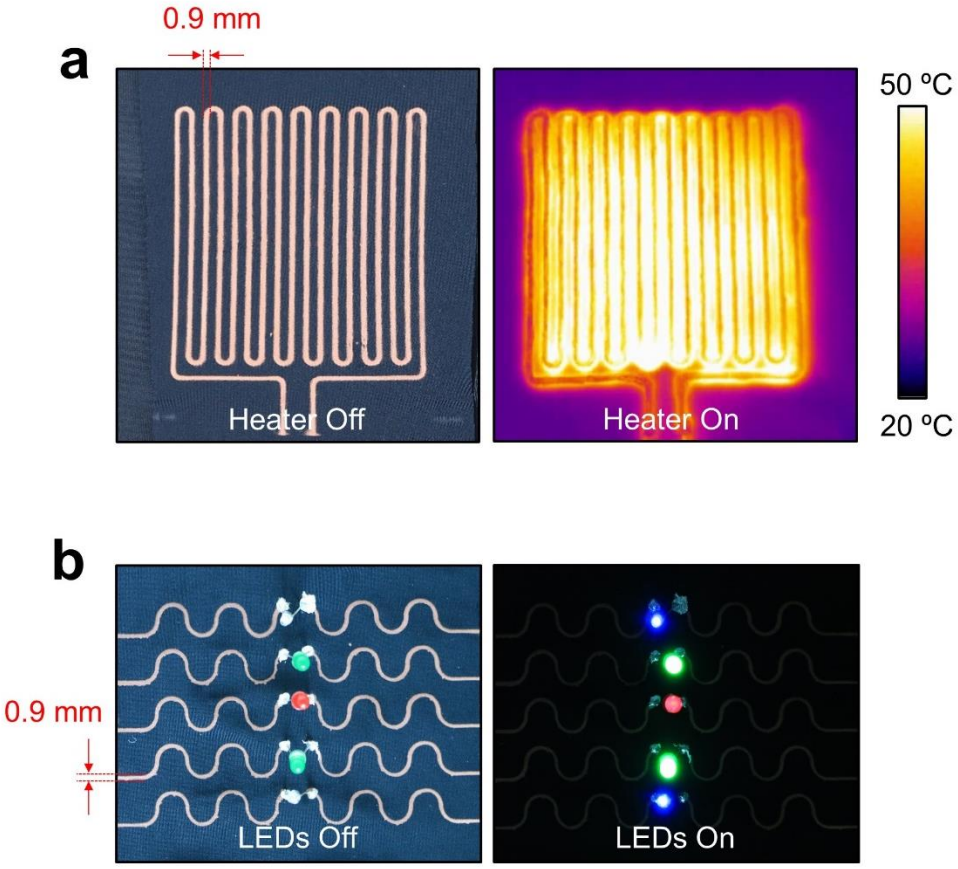

Figure S10. Examples of constructing e-textiles into (a) a resitive heater and (b) LEDs at the optimal operational condition.

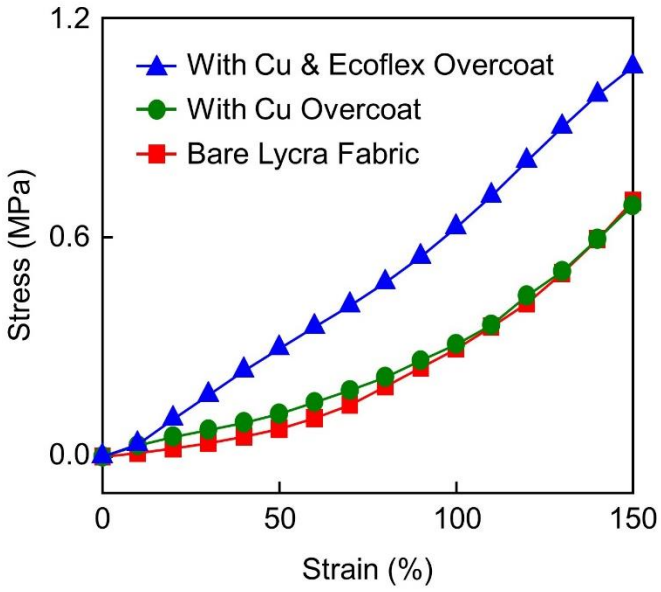

Figure S11. Mechanical modulus of a test unit with and without the presence of the Ecoflex overcoat as compared to the bare Lycra fabric.

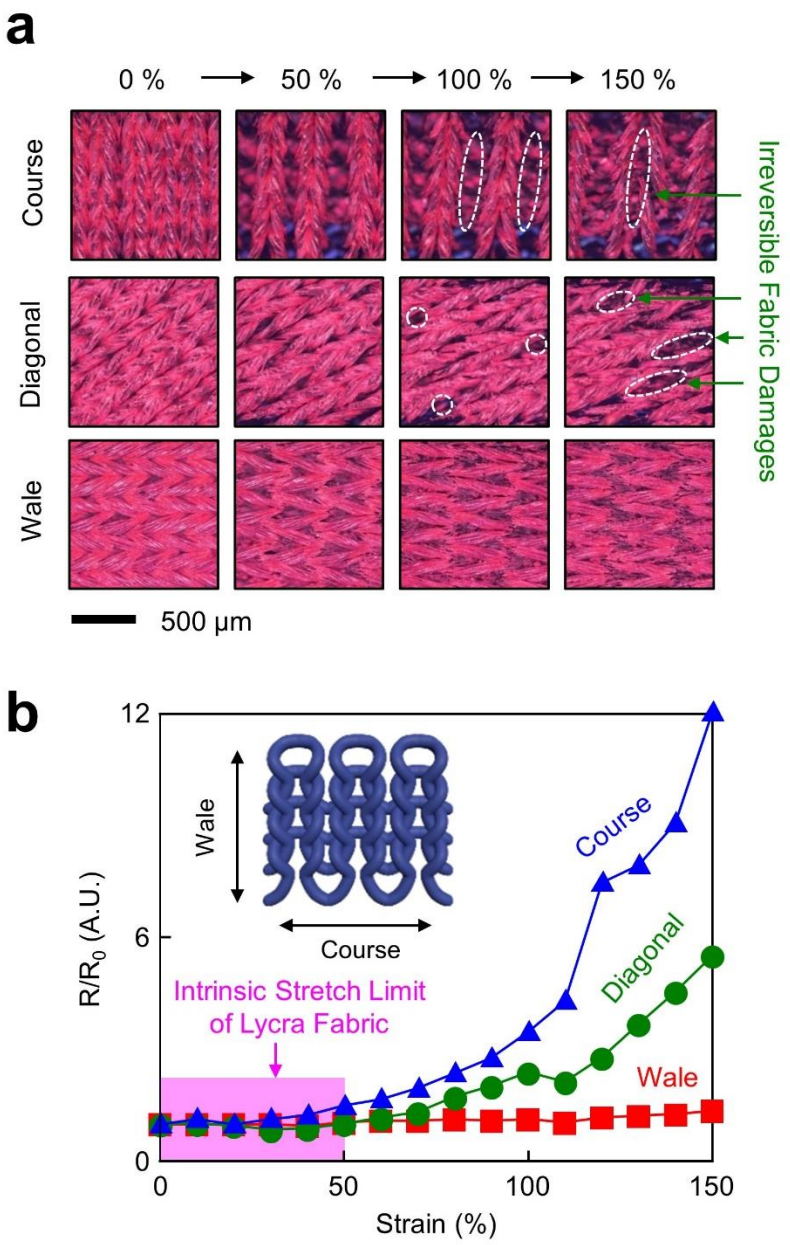

Figure S12. (a) Microscope images of a test unit under stretching up to 150% along wale, diagonal, and course directions from the top. The white dotted circles denote the irreversible fabric damages. (b) R/R_0 of a test unit under stretching up to 150%.

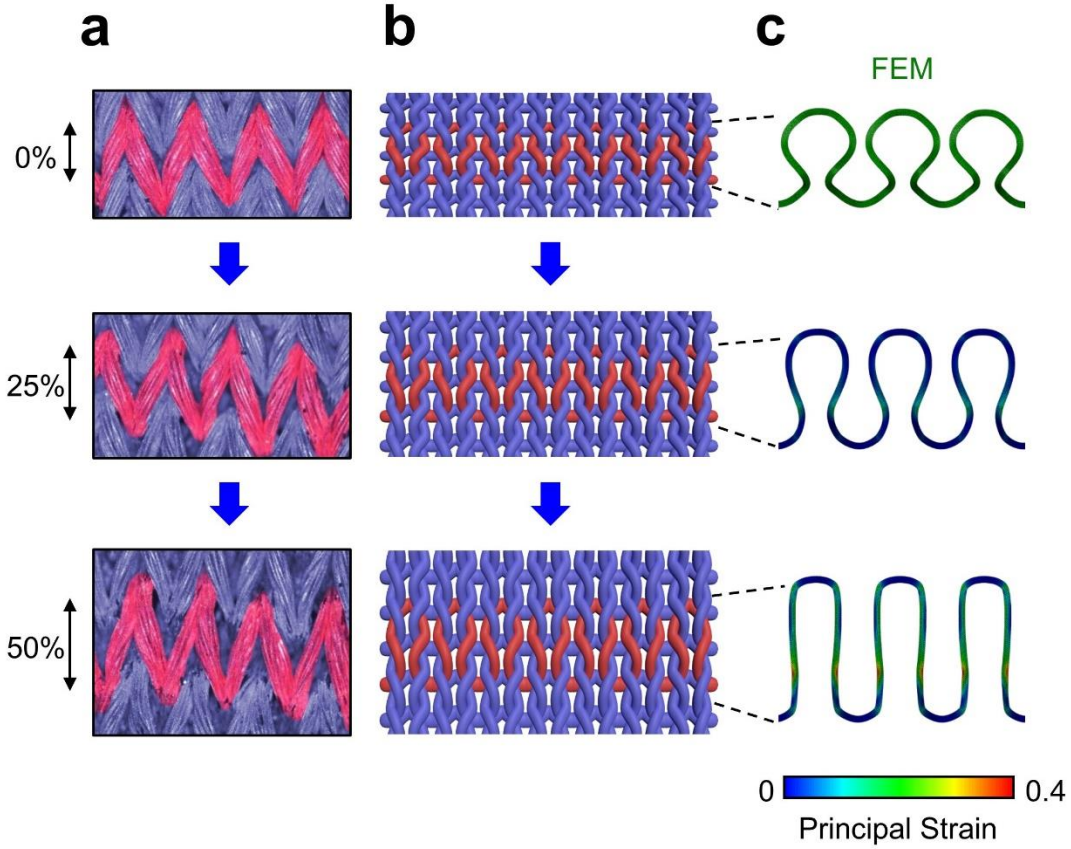

Figure S13. (a) Colored microscopy images, (b) schematic illustration, and (c) FEM results of the single filamentary column in a Lycra fabric under stretching up to 50% along wale direction.

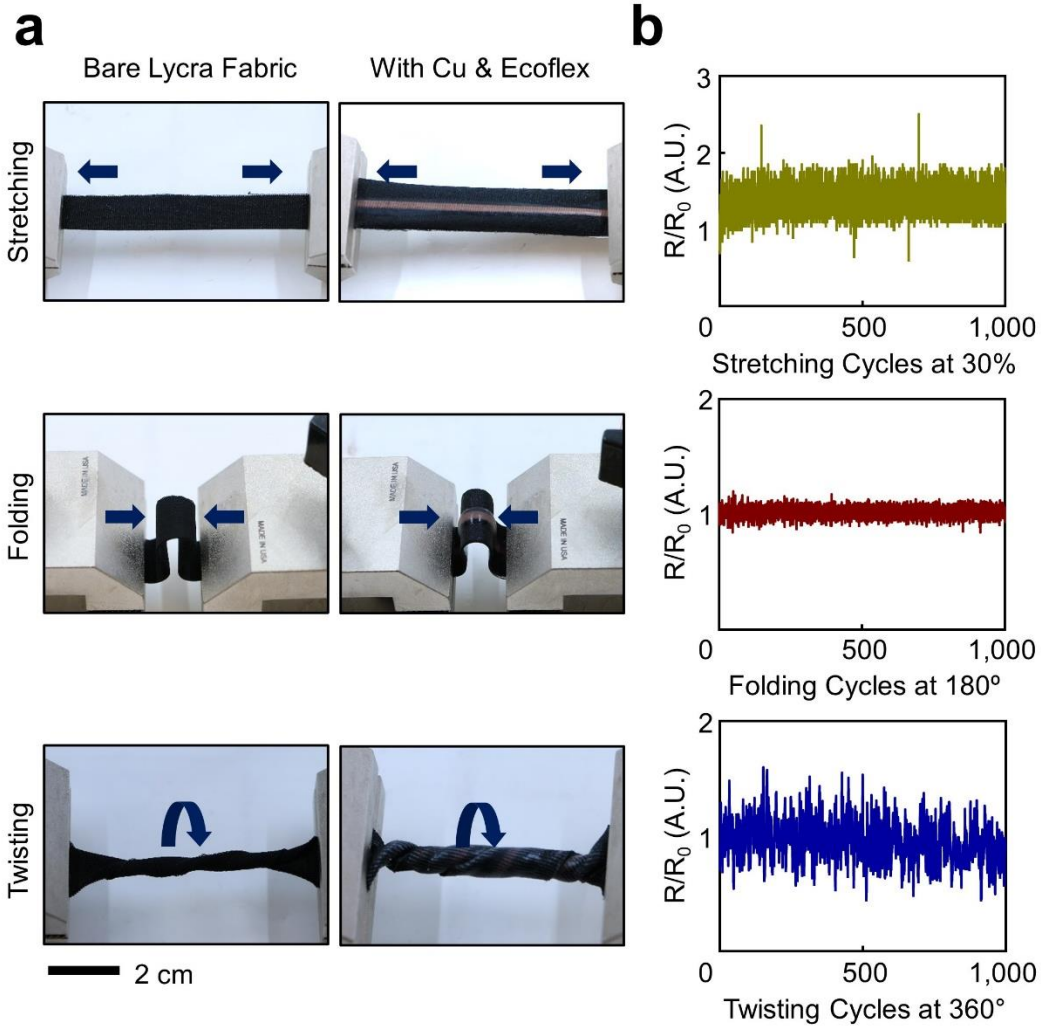

Figure S14. (a) Photographs of a test unit in a Lycra fabric with (left panel) and without (right panel) the presence of the Cu overcoat and Ecoflex overcoat under stretching, folding, and twisting from the top. (b) R/R_0 of a test unit under 1,000 cycles of stretching, folding, and twisting from the top.

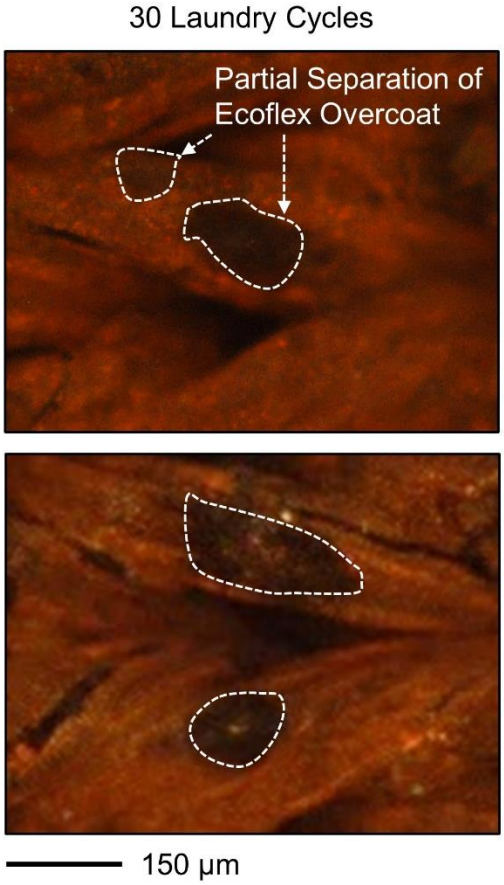

Figure S15. Representative microscope images showing the partial separation of the Ecoflex overcoat following a total of 30 laundry cycles.

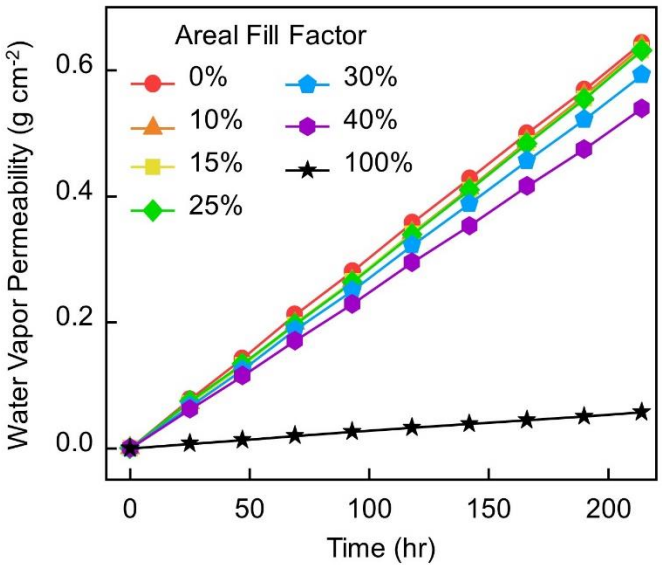

Figure S16. Water vaper permeability of the e-textiles that exhibit different areal fill factors of the Ecoflex overcoat ranging from 0 to 100%.

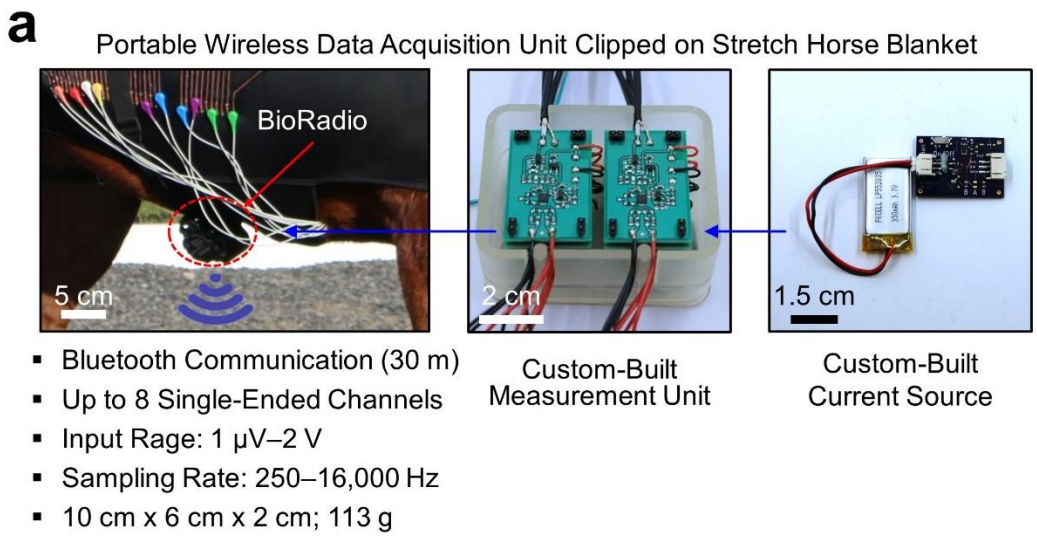

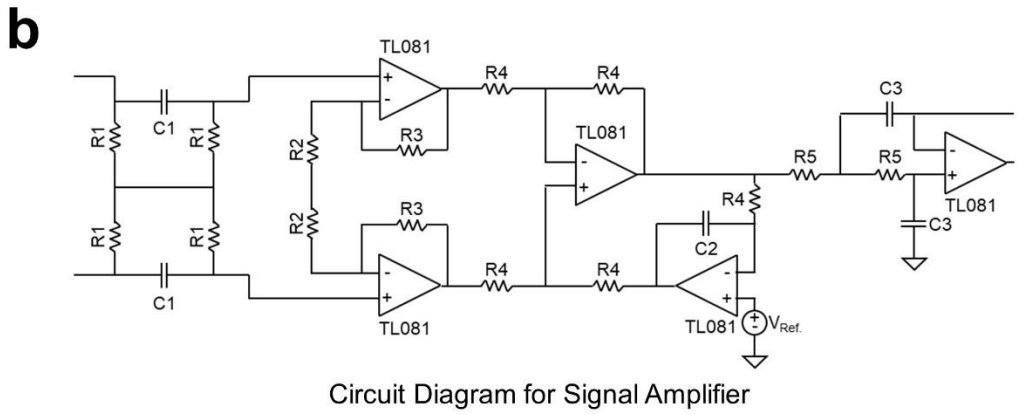

Circuit Diagram for Current Source

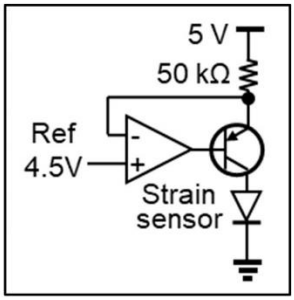

Components of ECG/EMG Amplifier

ECG	EMG
R1 = 10 MΩ	R1 = 10 MΩ
R2 = 500 Ω	R2 = 500 Ω
R3 = 50 kΩ	R3 = 50 kΩ
R4 = 10 MΩ	R4 = 150 kΩ
R5 = 100 kΩ	R5 = 20.5 kΩ
C1 = 0.33 μF	C1 = 1.6 nF
C2 = 1 μF	C2 = 100 nF
C3 = 10 nF	C3 = 10 nF

Figure S17. (a) Photographs of the custom-built portable data acquisition unit (left panel) that includes a custom-assembled measurement unit (middle panel) and a custom current source with a battery (right panel). (b) Circuit diagrams of the custom-made signal amplifier (top panel) and current source (bottom left panel), along with the components details for ECG and EMG (bottom right panel).

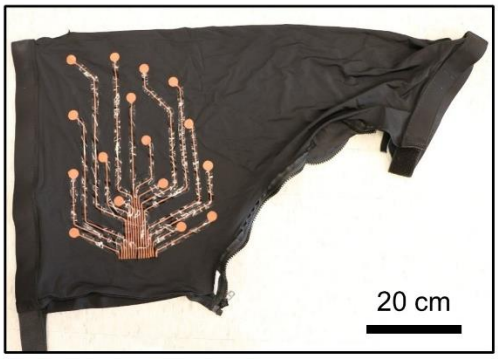

- Full Zip Blanket Hood
- Stretchable Lycra

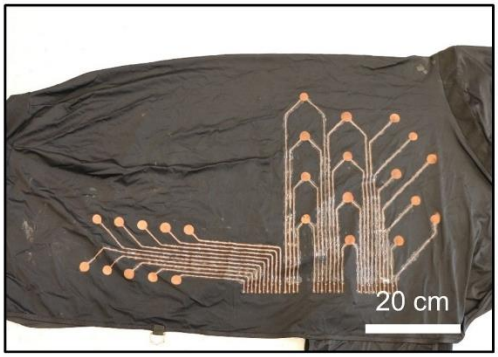

- Faceless Pull-On Full Body Blanket
- Stretchable Lycra

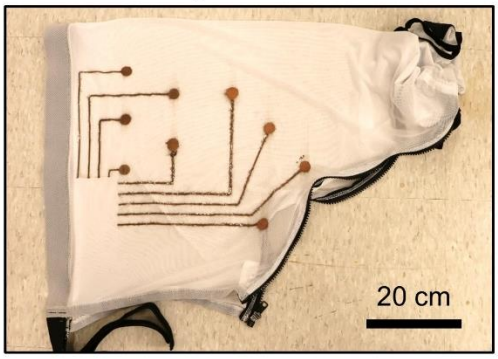

- Mesh Full Zip Blanket Hood
- Polyester (Polar Fleece)

Figure S18. Photographs of several different e-textiles in various types of commercial stretch horse blankets, including full zip slicker hood (Lycra), faceless pull-on full body slicker (Lycra), and mesh full zip slicker hood (polyester) from the top.

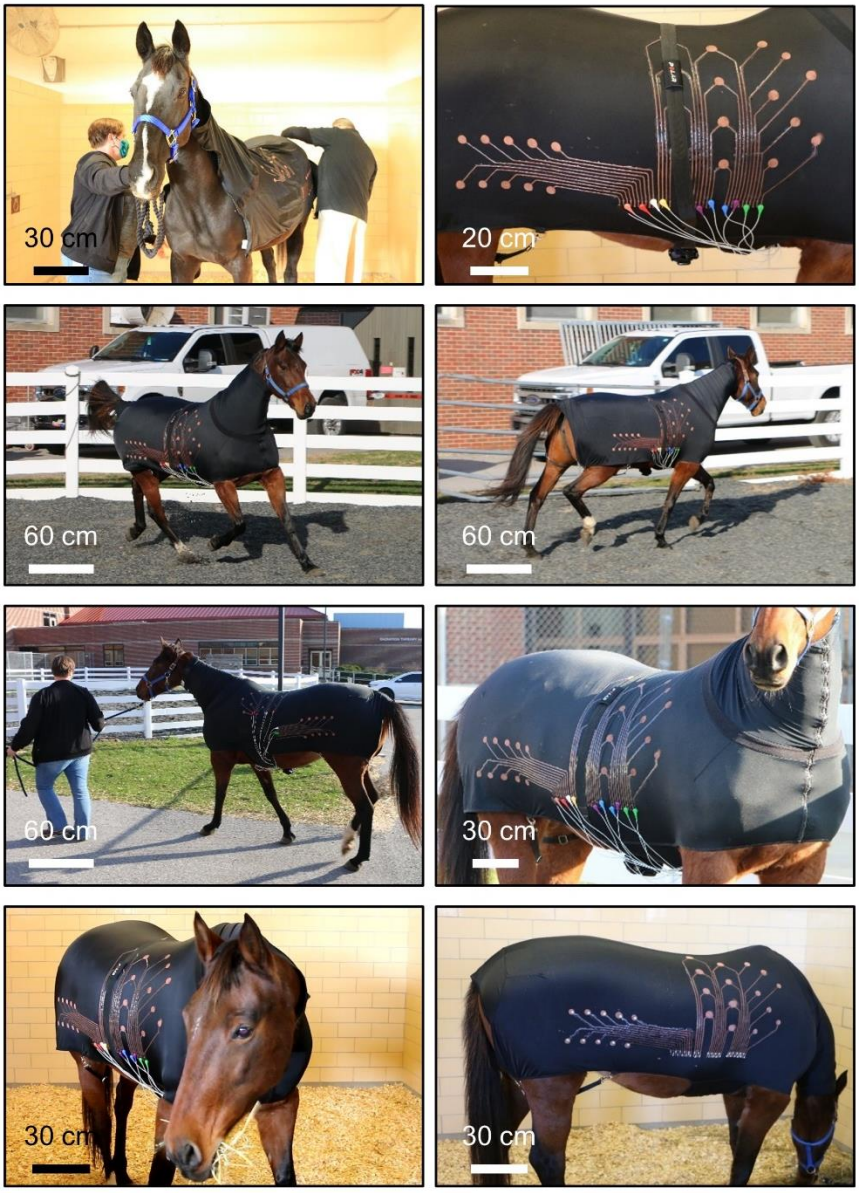

Figure S19. Photographs of a horse in a custom e-textile while freely walking, trotting, and galloping in a round pen or resting and eating in a stall.

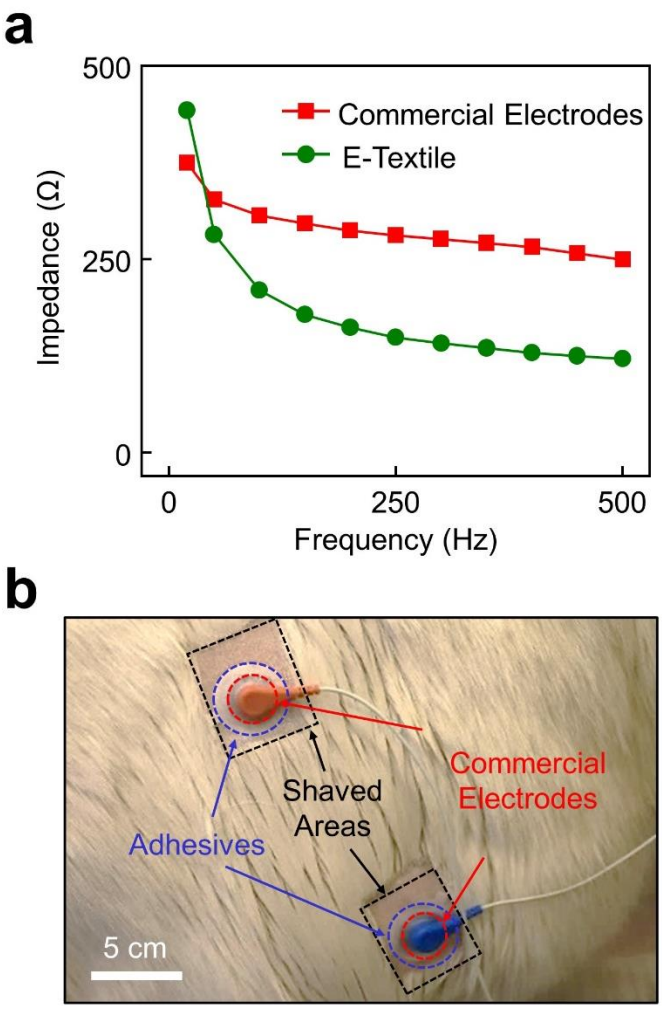

Figure S20. (a) Impedance measurement of the recording electrodes in e-textiles (green dotted line) as compared to commercial recording electrodes (red dotted line). (b) Photograph of the conventional recording electrodes on the skin of a horse after shaving haircoat.

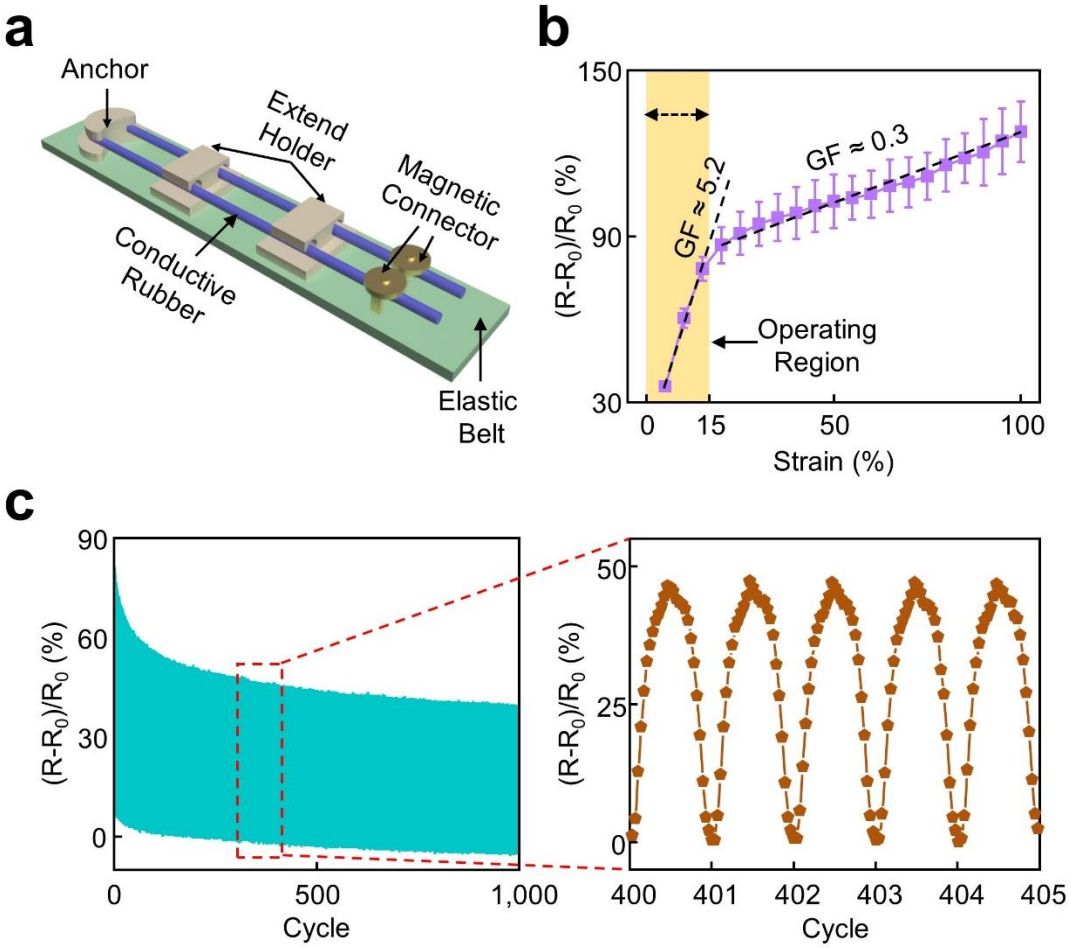

Figure S21. (a) Schematic illustration of the strain gauge. (b) Measurement of the gauge factor at the applied strain up to 100%. (c) R/R_0 of the strain gauge.

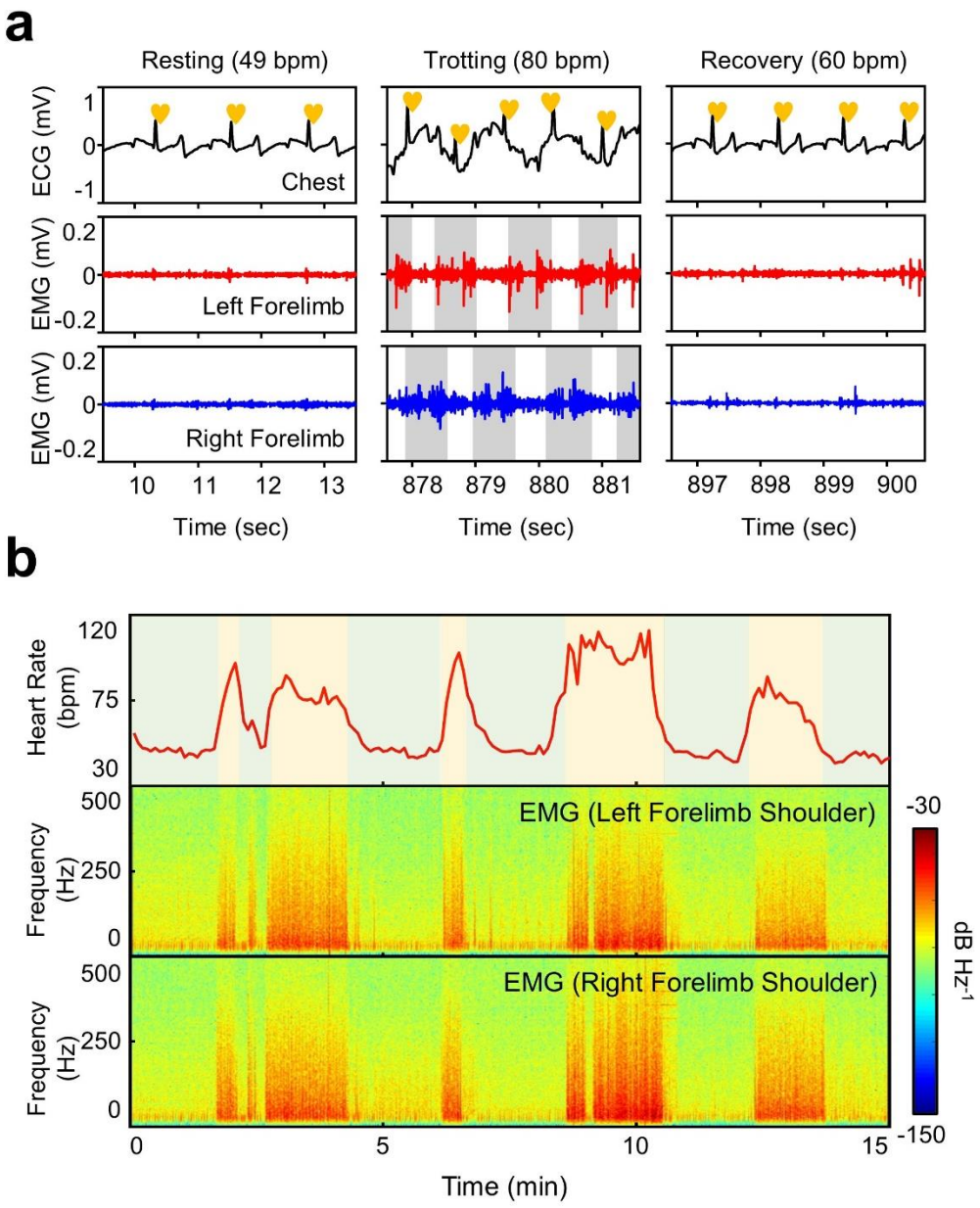

Figure S22. (a) Measurement results of ambulatory ECG and EMG signals obtained from the chest and forelimb shoulder of a horse in a round pen for 15 minutes while trotting, walking, and resting in a random order. (b) Corresponding time-series data, spectrograms and spectral information. The colors indicate the amplitude spectral density.

Movie Captions

Movie S1. Real-time video of the dual regime spray process.

Movie S2. Real-time video of the spray flow at V_C = 0−100 m sec^{-1}.

Movie S3. Real-time video of a horse in ambulatory health monitoring.